Electromechanical impedance temperature compensation and bolt loosening monitoring based on modified Unet and multitask learning

Fei Du, Shiwei Wu, Chao Xu, Zhaohui Yang, and Zhongqing Su

***Abstract*—Bolts are frequently subjected to loosening due to time varying external loads during service. The electromechanical impedance (EMI) technique based on piezoelectric ceramic wafers (PZT) is sensitive to the initial bolt preload looseness. However, the change in environmental temperature has a great effect on EMI monitoring. Deep convolutional neural network (CNN) is a promising technique for EMI monitoring. Nevertheless, it is difficult to train a deep CNN with limited training data to accurately identify damages under a wide range of temperature variations. To this end, this study proposes a multitask CNN for identifying bolts loosening. The network consists of a temperature compensation subnetwork to compensate for the temperature effect, and a lightweight damage identification subnetwork to identify bolt loosening states. The temperature compensation subnetwork is a modified Unet, and both the impedance and temperature are used as its input. The damage identification subnetwork is connected in series behind the temperature compensation subnetwork. A multiloss function is proposed in which a TV regularizer is used. Experimental results show that the validation accuracy of the multitask network is 97.71% when the network is trained by only about 30 samples from each loosening state. Moreover, the generalization abilities of the proposed multitask model to unexpected temperatures and bolt torques are investigated. The model is interpreted by the integrated gradients method, and is also compared with single-task damage identification CNNs. It is proved that the multitask network trained by limited samples can achieve accurate damage identification in temperature varying environments.**

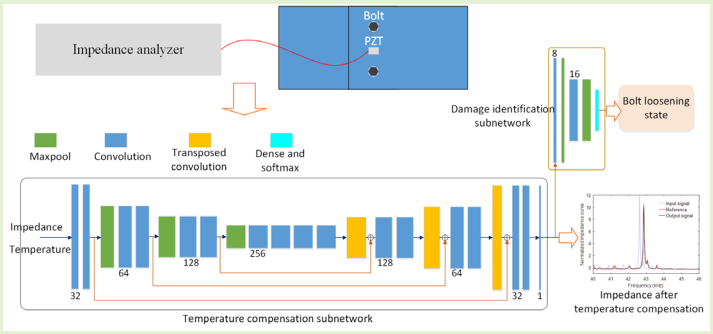

***Index Terms*—Electromechanical impedance, Deep convolutional neural networks, bolt loosening, Structural health Monitoring, Multitask learning.**

I. Introduction

MONITORING the health state of engineering structures, especially aerospace structures and civil engineering structures, is crucial to ensure their reliability and safety. For example, bolt connections in engineering structures usually bear large loads. However, bolts are frequently subjected to loosening due to time varying external loads during service. Bolts loosening may lead to the failure of the entire structure[1]. Structural Health Monitoring (SHM) technologies are the process of acquiring and analyzing data from onboard sensors to evaluate the health of a structure[2]. In addition to preventing catastrophic failure, it also leads to a significant reduction in maintenance costs, enhancement of structural integrity as well as reduction of inadvertent downtime of plants [3].

The electromechanical impedance (EMI) technique based on piezoelectric ceramic wafers (PZT) is commonly used for structural health monitoring[4-6]. In this technique, piezoelectric sensors are pasted on the structure. Then mechanical impedance of the structure can be evaluated by measuring the electrical impedance of the PZT sensor. The change of impedance can be used to assess the damage to the structure. The EMI method is sensitive to the initial damage of the structure and is suitable for complex structures. In practical application, the root mean square deviation (RMSD) and correlation coefficient (CC) of the real part of impedances before and after damage are often used as the damage indexes[4, 5], since the real part of the impedance is sensitive to structural damage.

In practice, the service temperature of engineering structure changes constantly, which leads to the changes of material characteristics of the piezoelectric sensor, the adhesive layer and the measured structure[7, 8]. In addition, the effect of

This study is supported by the National Natural Science Foundation of China (Grant No. 51705422). This study is also supported by Key Research and Development Program of Shaanxi (Program No.2021ZDLGY11-10), and Science, Technology and Innovation Commission of Shenzhen Municipality (JCYJ20190806151013025). *(Corresponding authors: Fei Du and Zhaohui Yang.)*

F. Du, S. Wu and C Xu are with School of Astronautics, Northwestern Polytechnical University, Xi'an, 710072, China and Yangtze River Delta Research Institute of Northwestern Polytechnical University, Taicang, Jiangsu, China (e-mail: dufei@nwpu.edu.cn; wushiwei@mail.nwpu.edu.cn; chao_xu@nwpu.edu.cn).

Z. Yang is with School of Aeronautics, Northwestern Polytechnical University, Xi'an, 710072, P.R. China. (e-mail: zhaohui@nwpu.edu.cn).

Z. Su is with Department of Mechanical Engineering, The Hong Kong Polytechnic University, Kowloon, Hong Kong and School of Astronautics, Northwestern Polytechnical University, Xi'an, 710072, China (e-mail: zhongqing.su@polyu.edu.hk).

temperature is also closely related to the thickness of the adhesive layer and excitation frequency[8]. As a result, the frequency and amplitude of resonance peaks of the measured EMI change with temperature. Therefore, the temperature effect must be compensated. Sun et al [9] first proposed to use cross correlation to compensate for the horizontal shift caused by temperature variation. Park et al [7] presented a damage metric and compensated for the horizontal and vertical shifts by minimizing the value of the damage metric. Koo et al[10] proposed an effective frequency shift method (EFS) for compensating temperature effects. The EFS is defined as the horizontal frequency shift corresponding to the maximum cross-correlation with the reference impedance. Moreover, the EFS method was used for impedance-based structural health monitoring of 2024-T3 aluminum panels under varying temperatures[11]. Wandowski et al. [12] further proposed a method to compensate horizontal frequency shift using CC and vertical amplitude shift using RMSD. Recently, Rabelo et al.[13] proposed a temperature compensation technique based on a hybrid optimization method associated with different damage metrics. However, the frequency shifts that resulted from temperature variations are not constant over the entire frequency range but increased with the frequency[14]. Gianesini [15] further observed that the temperature dependences of the vertical shifts are quadratic. Moreover, when the temperature and frequency ranges are extremely wide, the compensation results may lose efficiency since the frequency shifts follow a non-linear trend [16].

Machine learning methods are frequently used to achieve accurate identification of damage under temperature variations. Min[17] established a multilayer perceptron (MLP) for damage identification by EMI considering temperature effects. The multi-input of the MLP are CC values obtained from multiple frequency subranges compensated by EFS. Huynh et al[18] proposed a principal component analysis (PCA)-based algorithm to filter out temperature effects on EMI monitoring. A PCA-based temperature effect filtering model is established to filter out the temperature effects of the damage index matrix. Meanwhile, Huynh et al[19] developed a temperature compensation method based on radial basis function network (RBFN). In this method, the RBFN is trained with the impedance signals measured from the intact structure under various temperatures. Thereby, reference impedance signal at any temperature can be estimated by the RBFN to calculate the damage index. However, the RBFN is only applicable to the impedance signals from one specified damage state such as the healthy state. It can be concluded that the above traditional machine learning methods for damage identification still rely on damage indexes. Nevertheless, for bolt loosening monitoring, there are usually multiple damage states, and it is difficult to accurately distinguish the different states by damage indexes.

Deep convolutional neural networks (CNN) have brought about breakthroughs in processing images, video, speech and audio, and have been used in many other domains, such as medical image recognition[20], bioelectric signal processing[21] and fault diagnosis[22]. At present, increasingly more research efforts have also been put into the SHM domain[23]. However, training data are usually limited in the SHM domain. Zhang et al. [23] proposed a lightweight one dimension (1D) CNN, namely SHMnet, for the identification of loosening bolts in a steel frame. Time-domain data from repeated impact hammer tests were used for training. Additionally, multi-task learning[24] is to learn multiple tasks together to improve the learning of a model for each task by using the knowledge contained in all or some of the other tasks. Considerable achievements on MTL have been made in several fields such as image processing[25], fault diagnosis[26] and SHM based on guided waves[27].

Recently, CNNs have been applied in EMI-based damage monitoring. Choy[28] converted the 1D EMI signals to two-dimensional(2D) color images by repeat the 1D signals along the vertical direction of length. Then AlexNet and GoogLeNet were used to identify simulated damages. Almeida and Silva[29] established a 1D CNN and 2D CNN, both containing only one convolutional layer. For the 2D CNN, the signals were divided into segments and stacked to construct 2D images to be used as input. Nevertheless, the highest accuracy for identifying the four damage types of metal plates is 88.95%. The main reason for the relatively low accuracy is that the image features cannot be extracted well by only one convolutional layer. De Oliveira et al. [30] developed a 2D CNN with three convolutional layers to identify simulated structural damages. The impedance signal is split into several parts followed by computing the Euclidean distances among them to form an RGB image. The testing accuracy of the 2D CNN is 100%. Nevertheless, the above research works did not consider temperature variation. de Rezende et al[31] established a 5-layer 1D CNN containing one convolutional layer for the identification of simulated damage under three temperatures(0 °C, 10 °C and 20 °C). In fact, the temperature of the actual service environment usually varies continuously. It can be concluded that CNN is a promising technique for damage monitoring based on EMI. However, the effect of temperature variation on EMI has not been fully considered. In addition, there is usually a very limited amount of data available for training deep CNNs in EMI monitoring.

To address the above research gaps, this paper proposes a multitask CNN for accurately identifying the loosening of bolts under a wide range of temperature variations with limited training data. A temperature compensation subnetwork based on a modified Unet is established to compensate for the temperature effect. Both impedance and temperature are used as the input. Subsequently, a lightweight damage identification subnetwork is established to identify various bolt loosening states, and its input is the compensated impedance which is the output of the temperature compensation subnetwork. For the training of this multitask CNN, a multiloss function is proposed, and the tradeoff parameters of the loss functions of the two subnetworks are dynamically adjusted. Moreover, the generalization abilities of the proposed multitask CNN to unexpected temperatures and bolt torques are investigated. The proposed multitask CNN is finally verified by comparing with single task CNNs.

The content of this paper is arranged as follows. Section II introduces the theatrical backgrounds of EMI monitoring and CNN. Section III presents the multitask network and the multiloss function. The experimental process is shown in section IV. Section V presents the experimental results and

discussion. The study is concluded in section Ⅵ.

II. Theoretical Background

A. Analytical Model for EMI Monitoring of Damage

PZT wafers can convert electrical and mechanical energy to each other. When EMI is used for monitoring damage, a PZT wafer is usually bonded to the base structure, as shown in Figure 1a. The length, width and height of the wafer are l_a, b_a and t_a, respectively. In this case, the wafer is constrained by the base structure with structural stiffness k_{str}. This can be simplified to a model with $2k_{str}$ springs at each end of the PZT wafer [32], as shown in Figure 1b.

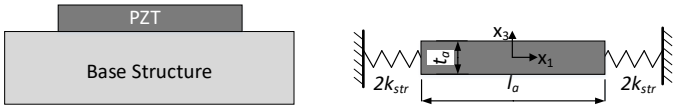

Fig. 1. Base structure with PZT wafer attached (a) actual structure (b) simplified model[32]

Based on structural vibration theory and theory of piezoelectricity, the electrical impedance of the PZT wafer in the simplified model can be expressed as[4, 24]

$$Z=\frac{1}{i\omega C}\left[1-k_{31}^2\left(1-\frac{1}{\frac{k_{str}}{k_{PZT}}+\frac{1}{2}\gamma l_a\cot\left(\frac{1}{2}\gamma l_a\right)}\right)\right]^{-1} \tag{1}$$

where $C=\varepsilon_{33}^T b_a l_a/t_a$ is the capacitance of the PZT, k_{31} is the E/M coupling factor, k_{PZT} is the stiffness of the PZT, $\gamma=\omega/c_a$ is the wavenumber in the PZT wafer, ε_{33}^T is dielectric constant at zero stress, ω is angular frequency, c_a is the sound speed.

According to Eq. (1), structural resonances will be reflected in the electrical impedance frequency spectra. In addition, the structural stiffness k_{str} changes when the structure is damaged, which will directly lead to changes in the resonance peak of the impedance. Therefore, the damage can be monitored by the impedance of the PZT. However, Eq. (1) does not take into account the effect of temperature. In fact, temperature directly affects the material characteristics, and thus the electrical displacement and strain of the PZT. In this case, the measured impedance signal will shift in frequency (horizontal shift) and change in amplitude (vertical shift) with the change of temperature[12].

In practical application of EMI, the damage state of a structure is usually determined by comparing the real parts of the impedance signals before and after the damage. The impedance measured from the intact structure is often called reference impedance. The root mean square deviation (RMSD) and the correlation coefficient (CC) are commonly used as damage indexes[33, 34]. However, in the case of temperature variation, RMSD and CC without temperature compensation will lead to false alarms [35].

B. Convolutional Neural Networks and Multitask Learning

Convolutional Neural Network (CNN) is a neural network that uses convolutional operations instead of general matrix multiplication. CNN can be used to process 1D sequence data or 2D image data. The convolutional layer is the core of the convolutional neural network.

1) 1D CNN

For 1D signals, a 1D convolution operation is used. In this case, the input feature of the convolution layer is a 2D tensor $X\in\mathbb{R}^{M\times D}$, where D is the number of channels and M is the length of the signal. The output feature is also a 2D tensor $Y\in\mathbb{R}^{M'\times P}$, where P is the number of output channels and M' is the length of the output feature. The convolution kernel is a 3D tensor $W\in\mathbb{R}^{U\times P\times D}$, where U is the size of the kernel. The output feature Y^P of the convolution layer can be calculated by

$$Y^P=W^P\otimes X+b^P \tag{2}$$

where $\otimes$ is the cross-correlation operation, b^P is the bias. The final output feature is usually obtained by a nonlinear activation function, as shown in the following Eq.

$$V^P=f\left(Y^P\right) \tag{3}$$

where $f(\bullet)$ is the nonlinear activation function. Recently, rectified linear units, ReLU is commonly used[36]. Convolutional operations have the characteristics of sparse interactions and parameter sharing, which effectively reduce the number of network weights and the complexity of the network[37].

Pooling layer is usually connected to convolutional layer. The pooling function uses the overall statistical characteristics of adjacent outputs at a location to replace the output at that location. Max pooling and average pooling functions are commonly used. Pooling operation can reduce the spatial resolution of input features, making the network have translation invariance and scaling invariance to the input[38].

2) Multitask Learning

Multitask Learning (MTL), a learning paradigm in machine learning, aims to jointly learn multiple related tasks so that the knowledge contained in a task can be leveraged by other tasks with the hope of improving the generalization performance of all the tasks [24]. In the context of Deep Learning, multitask learning is typically done with either hard or soft parameter sharing of hidden layers[39]. Hard parameter sharing is the most commonly used approach to MTL in neural networks[39]. It is generally applied by sharing the hidden layers between all tasks while keeping several task-specific output layers. Hard parameter sharing greatly reduces the risk of overfitting.

The loss function in the MTL generally yield the following empirical risk minimization formulation[40]

$$\min_{\theta^{sh},\theta^1,\cdots\theta^T}\sum_{t=1}^{T}c^t L^t\left(\theta^{sh},\theta^t\right) \tag{4}$$

where T is the number of tasks, θ^{sh} are the shared parameters between tasks and θ^t are task-specific parameters,

$L^t\left(\theta^{sh},\theta^t\right)$ is the loss functions of task t, and c^t is the static or dynamically computed weight of task t.

III. Framework of the Proposed Method

A. Input features

Both temperature and real part of impedance are used as input features. Each measured impedance signal is normalized using the Min-Max normalization method, as shown in the following equation.

$$\overline{Z}(\omega)=\frac{\mathrm{Re}\left(Z(\omega)\right)-\min\left(\mathrm{Re}\left(Z(\omega)\right)\right)}{\max\left(\mathrm{Re}\left(Z(\omega)\right)\right)-\min\left(\mathrm{Re}\left(Z(\omega)\right)\right)} \tag{5}$$

The temperature corresponding to each impedance signal is measured at the same time. In addition, the measured temperature is normalized by the following equation.

$$\overline{q}=\left(q-q_r\right)/10 \tag{6}$$

where q is the measured temperature, q_r is the reference temperature which is a fixed value for all damage states. Since a wide temperature range of 16-70°C is considered, the difference between the above two values is divided by 10. The normalized temperature $\overline{q}$ is repeated along the length to obtain a temperature vector $\overline{Q}$ so that its dimension is the same as the impedance signal. In this way, both the $\overline{Z}(\omega)$ and $\overline{Q}$ are used as input features.

B. Modified Unet-based temperature compensation subnetwork

The impedance signal changes significantly with damage states. Hence, the variation of impedance signal with temperature varies greatly from one damage state to another. A modified 1D Unet is established to compensate for the change of impedance signal caused by temperature variation at various damage states. This network is named the temperature compensation subnetwork. The output of the subnetwork should be the same as the impedance measured at the reference temperature. The architecture of the subnetwork is shown in Fig. 2, and the numbers of output channels of every convolutional layer are also displayed in the figure.

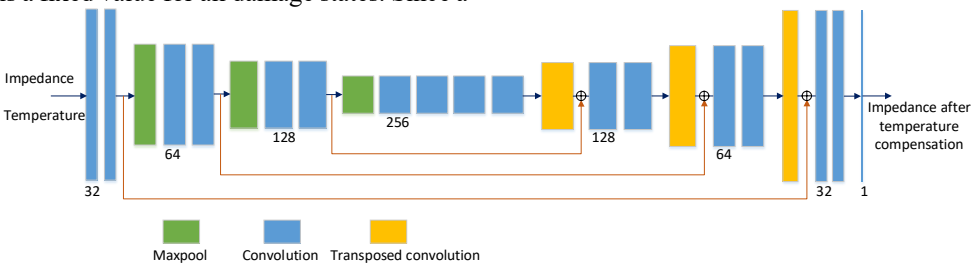

Fig. 2. The architecture of the temperature compensation subnetwork

The Unet[41] is a typical full convolutional neural network. Since the training dataset in EMI monitoring is generally small, the specific structure of the subnetwork after the modification is as follows.

(1) The contracting path contains three downsampling blocks. Each block consists of a maximum pooling layer and two convolutional layers, except that the third block contains four convolutional layers. Each convolutional layer is followed by a ReLU function. The number of output channels of the first convolutional layer of each block is twice the number of its input channels. The stride of the pooling layer is 2 for downsampling.

(2) The expansive path consists of three upsampling blocks, each containing one transposed convolutional layer and two convolutional layers. Each convolutional layer is followed by a ReLU function. The stride of the transposed convolutional layer is 2, while the number of its output channels is half of its input channel number.

(3) Three symmetric skip connections are used between the contracting and expansive paths. For the skip connections, residual learning formulation is adopted, i.e. each element of the corresponding Tensor is directly summed. This is different from reference[41]. This residual learning formulation reduces the number of channels in the following convolution layers, and we empirically find that this works better.

(4) The subnetwork contains a total of 17 convolutional layers. All the convolutional layers are equal-width convolutions with a kernel size of 3, except for the final output layer which has a convolution kernel of 1. Since the Batch Normalization layer is ineffective when the Batch Size is small [42], there is no BatchNorm layer in the subnetwork.

C. Multitask network for EMI damage identification

A damage identification subnetwork is connected in series behind the temperature compensation subnetwork, as shown in Figure 3. The input of this identification subnetwork is the output of the temperature compensation subnetwork, and the number of input channels is 1. Since only the compensated impedance needs to be classified, a lightweight CNN is adopted.

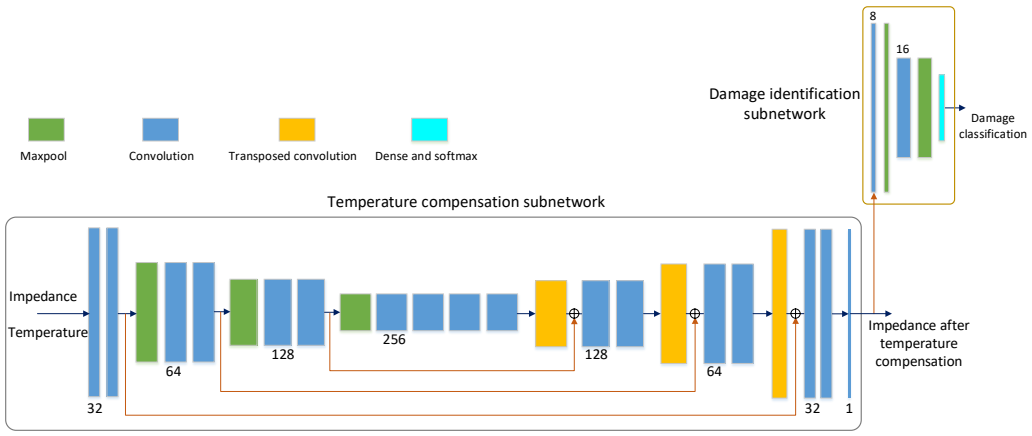

Fig. 3. The architecture of the damage identification multitask network

The specific structure of this subnetwork is as follows.

(1) The subnetwork consists of two convolutional layers, two maximum pooling layers and one linear layer. Each convolutional layer is followed by a ReLU function. The stride of the pooling layers is 2.

(2) The convolutional kernel sizes of the two convolutional layers are 7 and 5, respectively. In addition, the strides of the convolutional layers are 2.

(3) The dropout function is used before the linear layer to reduce the overfitting of the subnetwork. The softmax function is connected after the linear layer.

In this way, a multitask network is constructed for temperature compensation and damage identification. The network has two outputs, i.e. compensated impedance and classification of the damage.

D. Multiloss function

For the temperature compensation subnetwork, its output is the compensated real part of the impedance. Therefore, the mean square error loss function is used for this subnetwork, which can be expressed as

$$L_{MSE} = E\left[\left(\hat{\bar{Z}}(\omega) - \bar{Z}(\omega)\right)^2\right] \tag{7}$$

where $\hat{\bar{Z}}(\omega)$ is the compensated real part of impedance and $E(\bullet)$ is the calculation of mean value. Total variation (TV) regularizer can be used to constrain the smoothness of the difference between the predicted values and ground truth [25]. For 1D signals, gradient calculation becomes derivative calculation, and this loss function is shown in the following Eq.

$$L_{TV} = E\left[\left(\sigma(\omega)'\right)^2\right] \tag{8}$$

where $\sigma(\omega) = \hat{\bar{Z}}(\omega) - \bar{Z}(\omega)$. Hence, the loss function of the compensation subnetwork becomes the following Eq.

$$L_1 = L_{MSE} + \lambda_{TV} L_{TV} \tag{9}$$

where λ_{TV} is the tradeoff parameter of the TV regularizer.

For the damage identification subnetwork, the cross-entropy loss function is used, as shown in the following equation.

$$L_2 = -Y^T \log \hat{Y} \tag{10}$$

where Y is the ground truth of the distribution of labels and $\hat{Y}$ is the prediction distribution. The multitask model is trained as a whole, rather than the two subnetworks being trained separately. Hence, the multiloss function for the multitask network is

$$L = \lambda_1 L_1 + \lambda_2 L_2 \tag{11}$$

where λ_1 and λ_2 are the tradeoff parameters of the L_1 and L_2. The sum of λ_1 and λ_2 is 1.

IV. Experiment Validation

In this section, impedance signals of a two-bolt lap plate are measured under different temperatures and preloads using a single PZT wafer. Training and validation datasets are built to train and validate the proposed multitask network. Since the datasets are very important for the universality of deep learning, the specimen and the related parameters in the experiment were carefully selected.

A. Experimental rig and specimen

The two-bolt lap plate is shown in Figure 4. In aerospace structures, 3mm thick aluminum plate and M6 bolt are widely used. The bolts are steel M6 bolts of strength class 8.8. Flat shims were used in each bolted joint. The size of each aluminum plate is 120mm×80mm×3mm. In the middle of two M6 bolts, the PZT wafer is glued on the outer surface of an aluminum plate. The PZT is P5-H, and its size is 10mm×8mm×0.5mm.

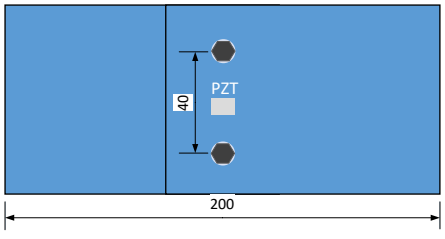

Fig. 4. Schematic diagram of the two-bolt lap plate (unit: mm)

An impedance analyzer of HIOKI IM3570 was used to measure the impedance of the PZT wafer. A digital torque wrench of STANLEY SD-030-22 was used to tighten the M6 bolts to the predetermined torques. An electric thermostatic drier 202-00A was used to control the environmental temperature of the specimen. A four-wire thermistor PT100 was used to precisely monitor the temperature inside the drier. The impedance data were measured after holding for 15 min at each temperature to ensure that the monitored environmental temperature is the same as that of the specimen.

B. Experimental procedure

A pre-sweep measurement of impedance was performed on the specimen using the HIOKI IM3570 to select the frequency range of the subsequent impedance measurement. At this time, the bolt torques were both 10Nm. The results show that the resonance peak amplitude of the real part of the impedance is relatively large within 40 kHz -50 kHz. Therefore, the frequency range of the subsequent impedance measurements was chosen to be 40 kHz - 46.3 kHz. In this case, there are 498 data points for the real part of the impedance signal.

A total of 9 bolt loosening states were measured and 382 samples were acquired in the experiments. The bolt torques in each loosening state are listed in Table 1. And the bolt torque of 8Nm was selected based on a Chinese National Standard[43]. The specimen was tightened three times for the 9 loosening states using the torque wrench. Bolt loosening state 9 is the healthy state. In the experiment, the temperature range of the samples is from 16°C to 70°C. The temperatures are not fixed values in every state except the reference temperature, and the temperature distribution of all samples is shown in Fig.5. In the temperature range of 25°C to 70°C, the number of samples is basically evenly distributed, while the number of samples below 25 °C is small. Note that the reference temperature is selected as 30℃.

TABLE I
THE LOOSENING STATES FOR THE IMPEDANCE EXPERIMENT

Loosening state	Torques of the two bolts
1	1 Nm, 1 Nm
2	1 Nm, 4 Nm
3	1 Nm, 8 Nm
4	4 Nm, 1 Nm
5	4 Nm, 4 Nm
6	4 Nm, 8 Nm
7	8 Nm, 1 Nm
8	8 Nm, 4 Nm
9	8 Nm, 8 Nm

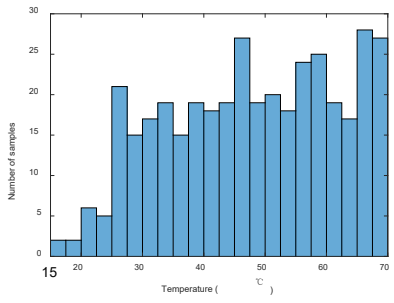

Fig. 5 The temperature distribution of all samples

280 samples were randomly divided into the training set and 102 samples into the validation set. This dataset is called the normal temperature dataset. In practical applications, unexpected extent of damage may occur in the monitored structure. The generalization ability of the developed multitask network to the temperature range of the training data was investigated. For this purpose, the impedance signals measured in the range of 25-60°C were taken as the training set, and the samples measured in the range of 16-25°C and 60-70°C were taken as the validation set. At this time, there are 271 samples in the training set and 111 samples in the validation set. This dataset is called the temperature generalization dataset.

In addition, an additional experiment on the same specimen was carried out to investigated the generalization ability of the model to unexpected bolt torques. 4 additional bolt loosening states were measured which are listed in Table 2. 50 samples per loosening state were acquired and the temperature range is from 24°C to 60°C. This dataset is called the torque generalization dataset. A self-made EMI monitoring device based on an AD5933 chip was used in the experiment. The frequency range is from 40kHz to 45kHz. Loosening states 10-13 can be seen as extensions of loosening states 1,3,7,9, respectively.

TABLE II
4 ADDITIONAL LOOSENING STATES

Loosening state	Torques of the two bolts
10	0 Nm, 0 Nm
11	0 Nm, 10 Nm
12	10 Nm, 0 Nm
13	10 Nm, 10 Nm

C. Neural network training and hyperparameter selection

The Adam optimization algorithm[44] was used for the training of the multitask network. Other hyperparameters for the network were listed in Table 3. The λ_1 and λ_2 values were dynamically adjusted in the training process. Since the damage identification is performed after temperature compensation, λ_1 is taken as 0.98 for the first 50 epochs, 0.96 for the 50th-100th epochs, and 0.92 for the final 100th-150th epochs. The multitask network was established and trained using the PyTorch platform.

TABLE III
HYPERPARAMETER VALUES

Hyperparameter	Value
epoch	150
batch size	6
learning rate	6e-4
λ_{TV}	0.02
λ_1	0.92-0.98
λ_2	0.08-0.02

V. RESULTS AND DISCUSSION

The results of the multitask network are shown in this section, and are compared with the results from the existing single task CNNs for SHM. The multitask network's generalization abilities to unexpected temperature and bolt torque were verified. Furthermore, the effect of frequency range was investigated.

A. Results of temperature compensation and damage identification

When the multitask network is trained by the normal temperature dataset, the loss and accuracy of the validation dataset are shown in Fig.6. The results are also compared with those obtained using two other loss functions. The first is the weights of λ_1 and λ_2 in Eq. (11) do not change dynamically, and their values are fixed at 0.92 and 0.08, which is called static loss. The other is that $\lambda_{TV}=0$, so the L_{MSE} is used for the temperature compensation subnetwork. In this case, the weights λ_1 and λ_2 are still dynamically adjusted. The results are also shown in Fig. 6 and Table 4. Note that the results in the table are the means and standard deviations of the three training results.

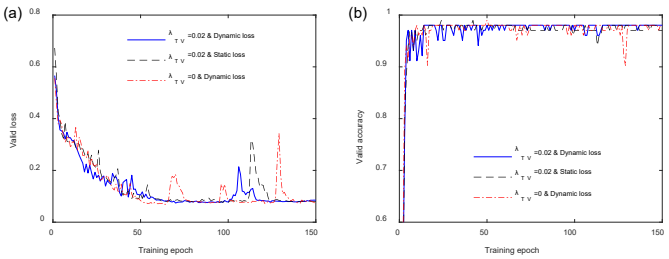

Fig. 6. A training process of the multitask network(a) Loss of the validation dataset (b)Accuracy of the validation dataset

TABLE IV
COMPARISON OF DIFFERENT LOSS FUNCTIONS

Loss function	Validation accuracy (Normal temperature dataset)
$\lambda_{TV}=0.02$ & Dynamic loss	97.71%±0.46%
$\lambda_{TV}=0.02$ & Static loss	96.73%±0.46%
$\lambda_{TV}=0$ & Dynamic loss	97.38%±0.46%

The results in Table 4 show that the validation accuracy using the proposed multiloss function is a little higher than those obtained by the other loss functions. It can also be seen from Fig.6 that, the accuracy and loss change more drastically during the training process when $\lambda_{TV}=0$.

The outputs of the temperature compensation subnetwork obtained by the three loss functions are compared with the corresponding impedance signals measured at the reference temperatures, as shown in Fig.7. The impedance signals shown are for loosening states 2, 4, 6, and 8. The input impedance signals in the four damages states are also shown in Fig.7, and the corresponding temperatures are 62.9℃, 44.0℃, 40.7℃, and 62.3℃, respectively. Note that there is an obvious difference between the impedance curves of loosening states 2 and 4 at the reference temperature. The main reason is that loosening states 2 and 4 are not exactly symmetrical. The input torque can be precisely controlled by a torque wrench, however, the torque-preload relationship is highly sensitive to friction that is affected by many factors[45]. Therefore, when these two bolts have the same torque, the preload is not exactly the same, resulting in different stiffness of the bolt joint. In addition, real engineering surfaces are rough. For bolt joints, different surface profiles will result in different contact pressure distributions and contact stiffness, even if the preloads are the same[46]. It can be concluded that when the two bolts have the same torque, their stiffness is not exactly the same. According to Eq. 1, the change in the stiffness of the base structure will lead to the change in the impedance curve. This is also true for loosening states 6 and 8.

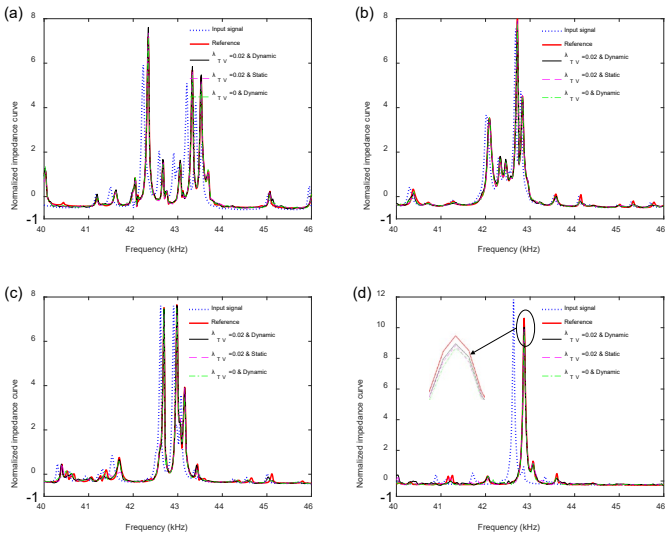

Fig. 7. Temperature compensation results under different bolt loosening states(a) Loosening state 2 at temperature 62.9℃ (b) Loosening state 4 at temperature 44.0℃ (c) Loosening state 6 at temperature 40.7℃ (d) Loosening state 8 at temperature 62.3℃

As can be seen from the results in Fig.7, the input impedance for each loosening state differs significantly from its corresponding impedance curve at the reference temperature. As the temperature increases, the resonance peak of the impedance shifts toward the lower frequencies and changes slightly in amplitude. As the reference temperature is 30℃, the changes shown in Fig. 7a and d are greater than those in Fig. 7b and c. After temperature compensation, the outputs all agree well with the impedance curves at the reference temperatures. It can also be seen from Fig.7d that the results obtained from the proposed loss function are in the best agreement with the impedance signals at the reference temperatures. On the other hand, it can be seen that the impedance curves differ greatly between the four loosening states.

To further interpret the proposed model, the Integrated Gradients method[47] is performed on the trained multitask model to attribute the model's outputs to its input signals. The Integrated Gradients method is conducted by Captum [48] which is an extensible library for model interpretability built on PyTorch. The results are displayed in Figs. 8 and 9.

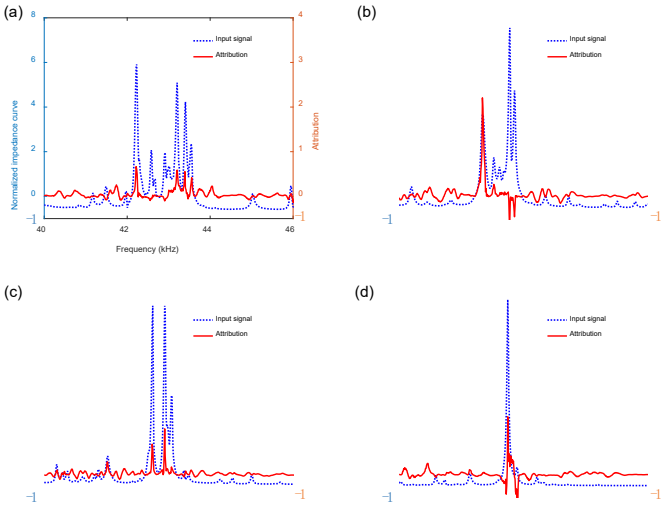

Fig. 8 Attribution for the damage classification (a) Loosening state 2 at temperature 62.9℃ (b) Loosening state 4 at temperature 44.0℃ (c) Loosening state 6 at temperature 40.7℃ (d) Loosening state 8 at temperature 62.3℃

Figure 8 shows the input attributions for the damage classification from the proposed multitask network. The input impedance signals in Fig.8 are the same as those in Figure 7. It can be seen the attribution values of several resonance peaks in an impedance signal are relatively large. Meanwhile, the attribution values of the rest of the signal are close to 0. It can be concluded that the damage classification by the multitask network is mainly based on the resonance peaks with large attribution values in the signal.

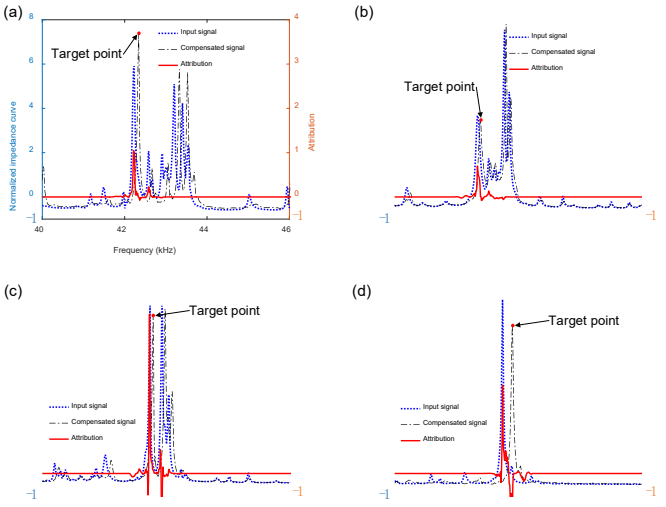

Fig. 9 Attribution for the compensated signal (a) Loosening state 2 at temperature 62.9℃ (b) Loosening state 4 at temperature 44.0℃ (c) Loosening state 6 at temperature 40.7℃ (d) Loosening state 8 at temperature 62.3℃

Figure 9 shows the input attributions for the temperature compensation from the multitask network. The input impedance signals in Fig 9 are the same as those in Figure 7. In the Captum, only a single value in the output of a neural network can be selected to compute attributions. This single value is called the target point. The target points in the output signals are shown in Fig.9. All the target points are the maximum points of one resonance peak in the signals. The attributions for the target points to their input impedance signals are also shown in Fig.9. It can be seen that the attribution values of the resonance peaks before frequency and amplitude shifts are dominant. In addition, the attribution values of the rest points in the input signals are 0. It can be concluded that the target points can be attributed to the maximum points of the resonance peaks before frequency and amplitude shifts. The above results explain how the network compensates the impedance signals for temperature.

B. *The generalization ability of the multitask network*

The multitask network is also trained and validated using the temperature generalization dataset. At this time, the samples measured at 25-60°C are taken as the training set, and those measured at 16-25°C and 60-70°C are taken as the validation set. The changes of loss and accuracy during the training of the network are shown in Fig. 10. The means and standard deviations of the accuracies are also listed in Table 5.

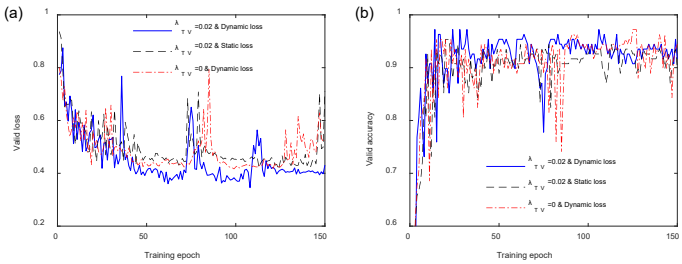

Fig. 10. A training process using the temperature generalization dataset(a) Validation Loss (b) Validation Accuracy

TABLE V
COMPARISON OF DIFFERENT LOSS FUNCTIONS USING THE TEMPERATURE GENERALIZATION DATASET

Loss function	Validation accuracy (Temperature generalization dataset)
$\lambda_{TV} = 0.02$ & Dynamic loss	93.21%±1.57%
$\lambda_{TV} = 0.02$ & Static loss	92.59%±2.00%
$\lambda_{TV} = 0$ & Dynamic loss	91.66%±2.73%

From Table 5, it can be seen that the validation accuracy is 93.21% with the proposed loss function, which is higher than those obtained by the other loss functions. Meanwhile, the standard deviation of the accuracy using the proposed loss function is smaller than those obtained by the other loss functions. Compared with the results shown in Fig. 6, however, the accuracy and the convergence speed shown in Fig. 10 are reduced and the loss value of the validation set is increased. Moreover, both the loss function and accuracy fluctuate more widely during the training process. The results demonstrate that the network can be effectively used to identify different loosening states outside its training temperature range. Note that only about 30 training samples are required for each loosening state in the training progress.

The outputs of the trained temperature compensation subnetwork are compared with the corresponding impedance signals at the reference temperatures, as shown in Fig.11. The impedance curves shown are for loosening states 2, 4, 6, and 8. The input impedance signals in the four damages states are also shown in Fig.11, and the corresponding temperatures are 62.9℃, 61.7℃, 61.7℃, and 60.2℃, respectively.

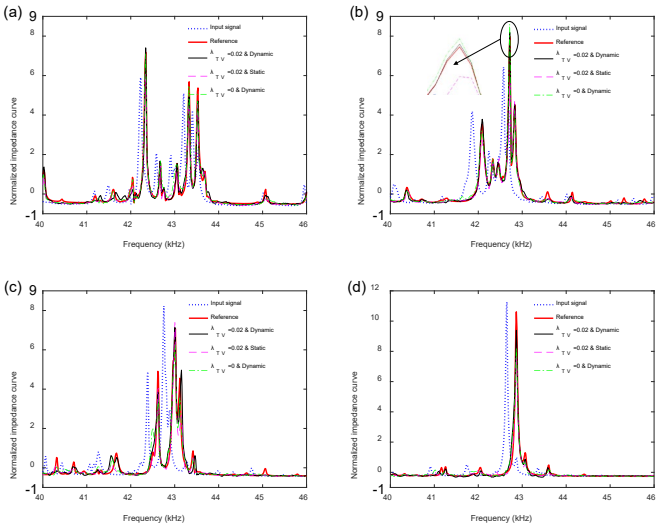

Fig. 11 Temperature compensation results for the temperature generalization dataset(a) Loosening state 2 at temperature 62.9℃ (b) Loosening state 4 at temperature 61.7℃ (c) Loosening state 6 at temperature 61.7℃ (d) Loosening state 8 at temperature 60.2℃

After temperature compensation, the outputs all agree with the corresponding impedance curves at the reference temperatures. It can also be seen from Fig. 11b that the results obtained from the proposed loss function are in the best agreement with the impedance signals at the reference temperatures. On the other hand, the deviations between the compensated impedance and reference impedance increase compared to the results shown in Fig. 7.

For the torque validation dataset, a comparison of the impedance signals from loosening states 10-13 and loosening states 1,3,7,9 is shown in Fig.12. It can be seen that the impedance signals measured by the AD5933 chip have vertical shifts. On the other hand, the distributions of the resonance peaks between loosening states 1 and 10,9 and 13 are similar, respectively. When the proposed multitask was validated by the torque validation dataset, the loosening states 1,3,7,9 were used as labels for the dataset shown in Table 2, respectively. At this time, the classification accuracy of the proposed model is 70.48%±4.48%. Note that the proposed CNN model was retrained using the training dataset with the frequency range of 40-45 kHz. It can be concluded that the proposed model can identify unexpected extent of loosening.

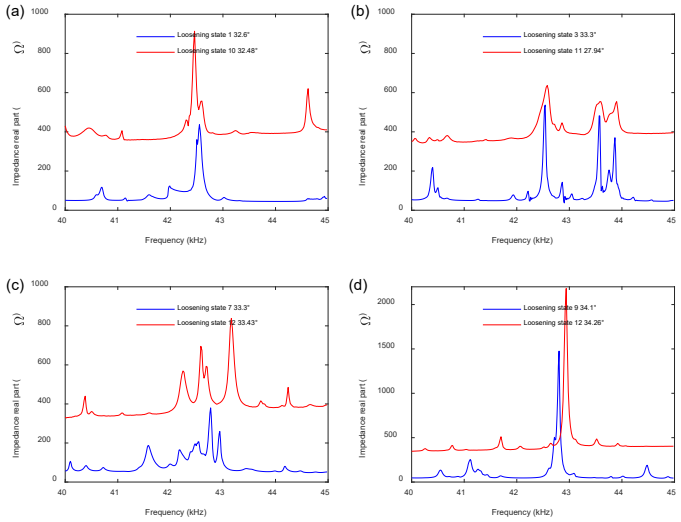

Fig. 12 The real parts of measured impedances (a) Loosening states 1 and 10 (b) Loosening states 3 and 11 (c) Loosening states 7 and 12 (d) Loosening states 9 and 13

C. Comparison with single-task CNNs

To verify the proposed multitask network, it was compared with the SHMnet[23] for bolt loosening detection and the 5-layer 1D CNN[31] for EMI monitoring. The results are listed in Table 6. In addition, a multistage-training process using the temperature compensation subnetwork and damage identification subnetwork was performed to compare with the multitask learning. In this process, the two subnetworks were not jointly trained but were separately performed. The temperature compensation subnetwork was trained using loss function L_1 and the final output was stored and used as the input of the damage identification subnetwork. The damage identification subnetwork was then trained using L_2. And the two networks as a whole was called as multistate-training network, the results are also listed in Table 6.

TABLE VI
COMPARISON OF DIFFERENT NEURAL NETWORKS

	Validation accuracy (Normal temperature dataset)	Validation accuracy (Temperature generalization dataset)	Parameters
Multitask network	97.71%±0.46%	93.21%±1.57%	1,005,674
Multistate-traiining network	97.06%±0.0%	90.43%±1.75%	1,005,674
SHMnet	91.18%±0.80%	64.56%±1.13%	13,168,068
5-layer 1D CNN	88.23%±1.39%	49.85%±2.58%	286,009

As can be seen from Table 6, the validation accuracy of the proposed multitask network is higher than that of the multistage-training network. The reason is that the multitask learning method improves identification accuracy. Table 6 also shows that the validation accuracy of the multitask network is higher than those of the SHMnet and the 5-layer 1D CNN. In particular, for the temperature generalization dataset, the

accuracy of the multitask network is about 30% higher than that of the SHMnet, and is 43% higher than that of the 5-layer 1D CNN. It is proved that the proposed model can be applied to datasets in which the temperatures are totally outside the range of the training dataset. Besides multitask learning, the main reason is that the change of impedance due to temperature variation can be effectively compensated by the temperature compensation subnetwork. This subnetwork is a full convolutional neural network of 17 convolutional layers, which has a strong feature extraction ability, and the measured temperatures were also utilized as input. After temperature compensation, bolt loosening states can be identified easily. It can be concluded that the proposed multitask network can achieve high accuracy with limited training data, and has good generalization ability in EMI damage identification.

It is important to select a frequency range that is sensitive to bolt loosening [17]. The frequency range used for the above results is 40-46.3 kHz. To verify the influence of the frequency range, the impedance signals in the frequency range of 40-44.3kHz , 40-48.1kHz and 43.8-50kHz are used for comparison. The data points for each signal are 348, 648 and 498, respectively. For the input impedance signals shown in Figure 7, the above three frequency ranges are displayed in Fig. 13. As can be seen from this figure, there are multiple resonance peaks in the frequency range of 40 kHz -50 kHz. In addition, the resonance peaks with larger amplitudes are mainly located in the 41.5-43.8 kHz frequency band.

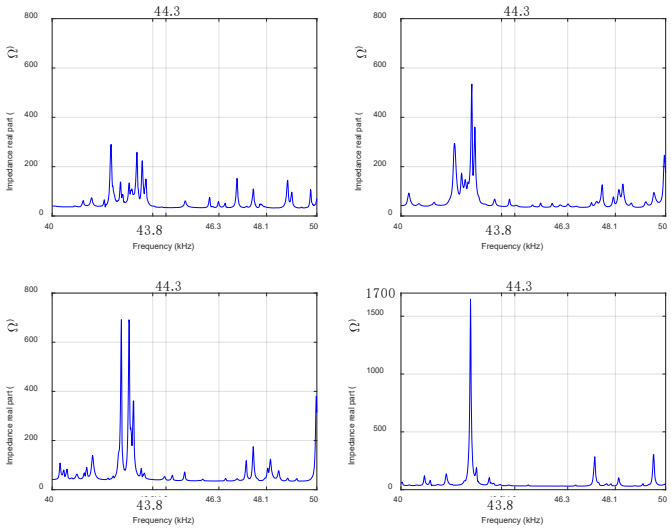

Fig. 13 Frequency ranges of the input signals before normalization (a) Loosening state 2 at temperature 62.9℃ (b) Loosening state 4 at temperature 44.0℃ (c) Loosening state 6 at temperature 40.7℃ (d) Loosening state 8 at temperature 62.3℃

The results of the multitask network and the SHMnet trained using the above frequency ranges are listed in Table 7.

TABLE VII
THE EFFECT OF FREQUENCY RANGE

	Frequency range /kHz	Validation accuracy (Normal temperature dataset)	Validation accuracy (Temperature generalization dataset)
Multitask network	40-48.1	97.38%±0.46%	93.83%±1.15%
	40-44.3	97.06%±0.0%	92.27%±2.19%
	43.8-50	97.47%±0.98%	91.34%±3.50%
SHMnet	40-48.1	93.79%±0.46%	68.47%±1.27%
	40-44.3	90.85%±1.22%	64.26%±5.22%
	43.8-50	93.46%±0.56%	68.47%±2.38%

From Table 7, it can be seen that for the multitask network, the variations of accuracy are less than 1% when using the frequency ranges of 40-48.1kHz and 40-44.3kHz. For the SHMNet, however, the variations of accuracy are about 3%. It can be concluded that the proposed multitask network is insensitive to the variation of the signal length. It can also be seen that when using the frequency range of 43.8-50kHz, the validation accuracies are almost the same as those obtained from the other frequency ranges. It can be deduced that the effect of different frequency bands is not significant.

VI. CONCLUSION

In this study, we proposed a multitask CNN for EMI monitoring of bolt loosening under wide temperature variation. The network consists of a temperature compensation subnetwork and a damage identification subnetwork. A multiloss function is presented for the training of the multitask network.

Experiments were conducted on a two-bolt lap plate with one PZT wafer attached to it. The results show that the validation accuracy of the multitask network is 97.71% when the network is trained by only about 30 samples from each loosening state. In addition, the change of impedance signal caused by temperature variation can be effectively compensated. Furthermore, the proposed multitask model was interpreted by the integrated gradients method. The results explained how the impedance signals are compensated and classified. Subsequently, a temperature generalization dataset is constructed, in which the temperature range of the training set is completely different from that of the verification set. In this case, the validation accuracy reached 93.21%. This indicates that the network can be applied well outside the temperature range of its training dataset. In addition, the generalization ability of the model to unexpected bolt torques was also investigated. It proved that the proposed model can identify unexpected extent of loosening.

The proposed multitask network is compared with the SHMnet and the 5-layer 1D CNN which are single-task CNNs. The results show that the validation accuracy of the multitask network is higher than those of the single-task CNNs. In particular, when the temperature generalized dataset is used, the accuracy is improved by at least 30% over the single-task CNNs. Besides multitask learning, the main reason is that the change of impedance due to temperature variation can be effectively compensated by the temperature compensation subnetwork. It is proved that the proposed network trained by

limited samples can achieve accurate damage identification in temperature varying environments.

REFERENCES

[1] T. Jiang, Q. Wu, L. Wang *et al.*, "Monitoring of Bolt Looseness-Induced Damage in Steel Truss Arch Structure Using Piezoceramic Transducers," *IEEE Sensors Journal,* vol. 18, no. 16, pp. 6677-6685, 2018.

[2] S. ARP, "Guidelines for Implementation of Structural Health Monitoring on Fixed Wing Aircraft," *Society of Automotive Engineers, Warrendale, Pa*, 2013.

[3] J. K. Agrahari, and S. Kapuria, "A refined Lamb wave time-reversal method with enhanced sensitivity for damage detection in isotropic plates," *Journal of Intelligent Material Systems and Structures,* vol. 27, no. 10, pp. 1283-1305, 2015.

[4] V. Giurgiutiu, *Structural Health Monitoring with Piezoelectric Wafer Active Sensors* 2ed., 225 Wyman Street, Waltham, MA 02451, USA: Elsevier, 2014.

[5] F. CR, and W. K, Structural health monitoring: a machine learning perspective, Chichester: John Wiley & Sons, 2013.

[6] D. E. Budoya, L. M. Campeiro, and F. G. Baptista, "Sensitivity Enhancement of Piezoelectric Transducers for Impedance-Based Damage Detection via a Negative Capacitance Interface," *IEEE Sensors Journal,* vol. 20, no. 23, pp. 13892-13900, 2020.

[7] G. Park, K. Kabeya, H. H. Cudney & D. J. "Inman. Impedance-based structural health monitoring for temperature varying applications". *JSME International Journal Series A Solid Mechanics and Material Engineering*, vol. 42, no. 2, pp. 249-258, 1999.

[8] Y. Yang, Y. Y. Lim & C. K. Soh. "Practical issues related to the application of the electromechanical impedance technique in the structural health monitoring of civil structures: I. Experiment". *Smart Materials and Structures*, vol. 17, no. 3, pp. 035008, 2008.

[9] F. P. Sun, Z. A. Chaudhry, C. A. Rogers, et al. "Automated real-time structure health monitoring via signature pattern recognition". in *Smart structures and materials 1995: smart structures and integrated systems. International Society for Optics and Photonics*, vol. 2443, pp. 236-247, 1995.

[10] K.-Y. Koo, S. Park, J.-J. Lee *et al.*, "Automated Impedance-based Structural Health Monitoring Incorporating Effective Frequency Shift for Compensating Temperature Effects," *Journal of Intelligent Material Systems and Structures,* vol. 20, no. 4, pp. 367-377, 2009.

[11] D. de Souza Rabelo, V. Steffen Jr, R. M. Finzi Neto, et al. "Impedance-based structural health monitoring and statistical method for threshold-level determination applied to 2024-T3 aluminum panels under varying temperature". *Structural Health Monitoring*, vol. 16, no. 4, pp. 365-381, 2017.

[12] T. Wandowski, P. H. Malinowski, and W. M. Ostachowicz, "Temperature and damage influence on electromechanical impedance method used for carbon fibre–reinforced polymer panels," *Journal of Intelligent Material Systems and Structures,* vol. 28, no. 6, pp. 782-798, 2017.

[13] D. S. Rabelo, K. M. Tsuruta, D. D. De Oliveira, A. A. Cavalini, R. F. Neto & V. Steffen. "Fault detection of a rotating shaft by using the electromechanical impedance method and a temperature compensation approach". *Journal of nondestructive evaluation*, vol. 36, no. 2, pp. 25, 2017.

[14] F. G. Baptista, D. E. Budoya, V. A. D. De Almeida, et al. "An experimental study on the effect of temperature on piezoelectric sensors for impedance-based structural health monitoring". *Sensors*, vol. 14, no. 1, pp. 1208-1227, 2014,

[15] B. M. Gianesini, N. E. Cortez, R. A. Antunes, et al. "Method for removing temperature effect in impedance-based structural health monitoring systems using polynomial regression". *Structural Health Monitoring*, vol. 20, no. 1, pp. 202-218, 2021.

[16] D. S. Rabelo, R. M. Finzi Neto, V. Steffen Jr. "Impedance-based structural health monitoring incorporating compensation of temperature variation effects". in *ABCM International Congress of Mechanical Engineering COBEM*. 2015.

[17] J. Min, S. Park, C.-B. Yun *et al.*, "Impedance-based structural health monitoring incorporating neural network technique for identification of damage type and severity," *Engineering Structures,* vol. 39, pp. 210-220, 2012.

[18] T.-C. Huynh, N.-L. Dang, and J.-T. Kim, "PCA-based filtering of temperature effect on impedance monitoring in prestressed tendon anchorage," *Smart Structures and Systems,* vol. 22, pp. 57-70, 2018.

[19] T.-C. Huynh, and J.-T. Kim, "RBFN-based temperature compensation method for impedance monitoring in prestressed tendon anchorage," *Structural Control and Health Monitoring,* vol. 25, no. 6, 2018.

[20] M. Loey, G. Manogaran, and N. E. M. Khalifa, "A deep transfer learning model with classical data augmentation and CGAN to detect COVID-19 from chest CT radiography digital images," *Neural Comput Appl*, pp. 1-13, Oct 26, 2020.

[21] F. Demir, V. Bajaj, M. C. Ince *et al.*, "Surface EMG signals and deep transfer learning-based physical action classification," *Neural Computing and Applications,* vol. 31, no. 12, pp. 8455-8462, 2019.

[22] J. Zhu, N. Chen, and C. Shen, "A New Deep Transfer Learning Method for Bearing Fault Diagnosis Under Different Working Conditions," *IEEE Sensors Journal,* vol. 20, no. 15, pp. 8394-8402, 2020.

[23] T. Zhang, S. Biswal, and Y. Wang, "SHMnet: Condition assessment of bolted connection with beyond human-level performance," *Structural Health Monitoring,* vol. 19, no. 4, pp. 1188-1201, 2019.

[24] Y. Zhang, and Q. Yang, "A Survey on Multi-Task Learning," *IEEE Transactions on Knowledge and Data Engineering*, pp. 1-1, 2021.

[25] S. Guo, Z. Yan, K. Zhang *et al.*, "Toward convolutional blind denoising of real photographs." pp. 1712-1722.

[26] Z. Liu, H. Wang, J. Liu *et al.*, "Multitask Learning Based on Lightweight 1DCNN for Fault Diagnosis of Wheelset Bearings," *IEEE Transactions on Instrumentation and Measurement,* vol. 70, pp. 1-11, 2021.

[27] B. Zhang, X. Hong, and Y. Liu, "Multi-task deep transfer learning method for guided wave based integrated health monitoring using piezoelectric transducers," *IEEE Sensors Journal*, pp. 1-1, 2020.

[28] A. W. Choy, "Structural Health Monitoring with Deep learning." pp. 557-60.

[29] J. H. L. Almeida, L. A. R. Lopes, M. A. B. Silva *et al.*, "Convolutional Neural Networks applied in the monitoring of metallic parts." pp. 1-8.

[30] M. A. De Oliveira, A. V. Monteiro, and J. Vieira Filho, "A New Structural Health Monitoring Strategy Based on PZT Sensors and Convolutional Neural Network," *Sensors (Basel),* vol. 18, no. 9, Sep 5, 2018.

[31] S. W. F. de Rezende, J. d. R. V. de Moura, R. M. F. Neto *et al.*, "Convolutional neural network and impedance-based SHM applied to damage detection," *Engineering Research Express,* vol. 2, no. 3, 2020.

[32] V. Giurgiutiu, and A. N. Zagrai, "Embedded Self-Sensing Piezoelectric Active Sensors for On-Line Structural Identification," *Journal of Vibration and Acoustics,* vol. 124, no. 1, pp. 116, 2002.

[33] L. M. Campeiro, R. Z. M. da Silveira, and F. G. Baptista, "Impedance-based damage detection under noise and vibration effects," *Structural Health Monitoring,* vol. 17, no. 3, pp. 654-667, 2017.

[34] R. Z. M. da Silveira, L. M. Campeiro, and F. G. Baptista, "Performance of three transducer mounting methods in impedance-based structural health monitoring applications," *Journal of Intelligent Material Systems and Structures,* vol. 28, no. 17, pp. 2349-2362, 2017.

[35] H. J. Lim, M. K. Kim, H. Sohn *et al.*, "Impedance based damage detection under varying temperature and loading conditions," *NDT & E International,* vol. 44, no. 8, pp. 740-750, 2011.

[36] A. Krizhevsky, I. Sutskever, and G. E. Hinton, "ImageNet classification with deep convolutional neural networks," *Communications of the ACM,* vol. 60, no. 6, pp. 84-90, 2017.

[37] I. Goodfellow, Y. Bengio, A. Courville *et al.*, *Deep learning*: MIT press Cambridge, 2016.

[38] W. Rawat, and Z. Wang, "Deep Convolutional Neural Networks for Image Classification: A Comprehensive Review," *Neural Comput,* vol. 29, no. 9, pp. 2352-2449, Sep, 2017.

[39] S. Ruder, "An overview of multi-task learning in deep neural networks," *arXiv preprint arXiv:1706.05098*, 2017.

[40] O. Sener, and V. Koltun, "Multi-task learning as multi-objective optimization." pp. 525-536.

[41] O. Ronneberger, P. Fischer, and T. Brox, "U-net: Convolutional networks for biomedical image segmentation." pp. 234-241.

[42] E. Hoffer, I. Hubara, and D. Soudry, "Train longer, generalize better: closing the generalization gap in large batch training of neural networks." pp. 1729-1739.

[43] "General rules of tightening for threaded fasteners", GB/T 16823.2-1997, The State Bureau of Quality and Technical Supervision of the People's Republic of China,1997.

[44] D. P. Kingma, and L. J. Ba, "Adam: A Method for Stochastic Optimization," in International Conference on Learning Representations, San Diego, USA, 2015.

[45] L. Zhu, J. Hong, X. Jiang, "On controlling preload and estimating anti-loosening performance in threaded fasteners based on accurate contact modelling", Tribology International, vol. 95, pp. 181-191, 2016.

[46] M. B. Marshall, R. Lewis, R. S. Dwyer-Joyce, "Characterisation of contact pressure distribution in bolted joints", Strain, vol. 42, no.1, pp.31-43, 2006.

[47] M. Sundararajan, A. Taly, Q. Yan. "Axiomatic attribution for deep networks", in International Conference on Machine Learning. PMLR, pp. 3319-3328, 2017.

[48] N. Kokhlikyan, V. Miglani, M. Martin, et al. “Captum: A unified and generic model interpretability library for pytorch”. *arXiv preprint arXiv:2009.07896,* 2020.

Fei Du received the Ph.D. degree in mechanical engineering from the Xi’an Jiaotong University, Xi’an, China in 2015. He is currently an Assistant Professor with the School of Astronautics, Northwestern Polytechnical University. His research interests include structural health monitoring based on impedance and guided waves, and machine learning methods for structural health monitoring.

Shiwei Wu received the B.S. degree in Aircraft design engineering from Northwestern Polytechnical University, Xi’an, China in 2021. He is currently pursuing the Master degree in aerospace Engineering at Northwestern Polytechnical University. His current research interests include deep learning methods for structural health monitoring.

Chao Xu received the Ph.D. degree in Aerospace Science and technology from the Northwestern Polytechnical University, Xi’an, China in 2007. He is currently a Professor with the School of Astronautics, Northwestern Polytechnical University. His research interests include structural health monitoring, structural dynamics of aerocraft and aerocraft structure design.

Zhaohui Yang received the Ph.D. degree in mechanical engineering from the Xi’an Jiaotong University, Xi’an, China in 2014. He is currently an Associate Professor with the School of Aeronautics, Northwestern Polytechnical University. His research interests include Aircraft structure optimization design and structural health monitoring.

Zhongqing Su received the Ph.D. degree from the The University of Sydney, Sydney, Australia in 2004. Prof. Zhongqing Su is Professor of Mechanical Engineering and Head of Department of Mechanical Engineering at the Hong Kong Polytechnic University (PolyU). He is the current Editor-in-Chief of journal Ultrasonics, and holds Changjiang Chair Professorship(Supporting Institution: at Northwestern Polytechnical University). His research interests lie primarily in the broad area of ultrasonics, structural health monitoring (SHM), wave propagation, sensors, non-destructive evaluation, smart materials and advanced composites.